Geomorphology 123 (2010) 154–164

Contents lists available at ScienceDirect

Geomorphology

journal homepage: www.elsevier.com/locate/geomorph

Delta distributary dynamics in the Skagit River Delta (Washington, USA): Extending, testing, and applying avulsion theory in a tidal system

W. Gregory Hood *

Skagit River System Cooperative, P.O. Box 368, LaConner, WA 98257, USA

ARTICLE INFO

Article history:
Received 11 March 2010
Received in revised form 8 July 2010
Accepted 12 July 2010
Available online 16 July 2010

Keywords:
Avulsion
Distributary dynamics
Skagit delta restoration

ABSTRACT

Analysis of historical aerial photos shows that Skagit Delta (Washington, USA) distributary dynamics are consistent with the Slingerland and Smith model of avulsion dynamics where the ratio of the water surface slopes of the two branches of a bifurcation predicts avulsion stability. This model was extended to predict distributary inlet (upstream) width and bankfull cross-sectional area. The water surface gradient ratio for a bifurcation pair predicted distributary width well; the lowest R^2 was 0.61 for the 1937 data points, but R^2 ranged from 0.83 to 0.90 for other year-specific regression lines. Gradient ratios were not constant over the historical record; from 1937 to 1972 the mainstem river channel lengthened by 1250 m in the course of marsh progradation, while distributary lengthening was comparatively negligible. Consequently, the gradient advantage of the distributaries increased and their channels widened. After the mainstem river terminus stabilized from 1972 to the present, the distributaries continued to lengthen with marsh progradation, so that distributary gradient advantage steadily declined and the distributaries narrowed. While distributary cross sections were not available for the historical period, they were surveyed in 2007 near the distributary inlets. Gradient ratio was more closely related to distributary inlet bankfull cross-sectional area ($R^2 = 0.95$) than to minimum distributary width for any photo year examined. Applying this form of analysis to Skagit Delta distributaries that have been dammed in the course of agricultural development suggests that their restoration to stabilize eroding marshes at their outlets and recover salmon migration pathways would be feasible without significant risk of full river avulsion.

1. Introduction

River distributaries are the framework upon which river deltas are built. As a river delivers sediment to its delta, the delta progrades and the river progressively divides into distributaries. Thus, the processes of delta and distributary network formation are inextricably interrelated (e.g., Edmonds and Slingerland, 2007; Stouthamer and Berendsen, 2007). The tight coupling between distributary and delta dynamics are illustrated by the classic description of delta lobe switching in the Mississippi Delta, where periodic river avulsion has caused the location of the active delta to shift hundreds of kilometers (Coleman, 1988). Distributary network geometry is potentially the most important factor controlling delta landforms (Coleman, 1988; Syvitski et al., 2005) and related hydrological, geological, and ecological processes. In addition to distributing river water over a delta, distributaries also distribute river-borne sediments, nutrients, stream wood, fish, and other aquatic organisms to estuarine and riverine floodplain wetlands along the distributaries. Because distributary network geometry in river-dominated estuaries affects the spatial distribution of estuarine salinity gradients and sedimentation patterns and these affect vegetation distribution, distributary geometry also affects wildlife distribution patterns through its effect on their habitat. Consequently, an understanding of distributary dynamics can be useful to sustainable habitat management (e.g., habitat protection and restoration) for important fish and wildlife in deltaic systems.

Human engineering significantly influences river distributaries and the growth and evolution of their associated deltas (Pasternack et al., 2001; Syvitski and Saito, 2007). Direct human modifications of distributary networks can include distributary blockage with dikes or distributary excavation to redirect river flows. Indirect impacts to distributaries result from system modifications such as dam construction, which moderates seasonal flood pulses and results in sediment retention in the dam reservoirs, or water withdrawals for irrigation or direct human consumption that effectively reduces the hydraulic size of the river basin (Syvitski, 2008). Sustainable system management requires better understanding of geoecological constraints on management sustainability and a better understanding of distributary network dynamics in particular.

River distributaries are primarily formed by avulsion (Slingerland and Smith, 2004) or channel bifurcation during mouth bar development and delta progradation (Edmonds and Slingerland, 2007).

* Tel.: +1 360 466 7282; fax: +1 360 466 4047.
E-mail address: ghood@skagitcoop.org.

0169-555X/$ – see front matter © 2010 Elsevier B.V. All rights reserved.
doi:10.1016/j.geomorph.2010.07.007

Avulsions are thought to be caused principally by channel aggradation and elevation above a floodplain, thereby creating a gradient advantage for a potential avulsion channel relative to the original channel; loss of channel capacity from channel infilling also contributes to avulsion (reviewed in Makaske, 2001; Slingerland and Smith, 2004). Slingerland and Smith (1998) modeled the critical slope ratios (water surface slope of an incipient avulsion relative to that of the river mainstem) that predicted avulsion fate. For medium-sand systems, the model predicted that ratios <1 would result in a failed avulsion where the incipient avulsion would ultimately fill with sediment. Ratios >5 would result in complete avulsion where the river would abandon its original course in favor of the higher gradient. Intermediate ratios were predicted to produce partial avulsion where two channels would persist indefinitely. However, in an empirical study of the lower Mississippi River, Aslan et al. (2005) found widespread gradient advantages in the river valley but few avulsions. Ratios of crossvalley to downvalley slope ranged from 16 to 110 and typically were >30. Major levee breaches did not capture river flow because of the widespread presence of floodbasin muds that inhibited avulsion. Instead, they observed avulsions in sand-filled abandoned river channels. The authors concluded gradient advantage may be necessary but not sufficient for avulsion. In addition to gradient advantage, they suggested erodable substrate, such as that present in active or abandoned floodplain channels, was key to successful avulsion. Other studies have likewise found reoccupation of paleochannels to be a common form of avulsion (reviewed in Slingerland and Smith, 2004).

The observations by Aslan et al. (2005) complemented rather than contradicted the avulsion model by Slingerland and Smith (1998). Resistance to erosion of a new channel means flow is generally more efficient in the old established channel. The amount of resistance is dependent on the type of material to be eroded (e.g., mud versus sand) and on the presence of vegetation that binds the soil. Energy for erosion of avulsion channels is proportional to channel gradient (e.g., Lorang et al., 2005). Overcoming the inherent efficiency of the mainstem channel and the resistance to erosion of the potential avulsion pathway requires a gradient advantage, i.e., an energetically favorable pathway. The greater the efficiency of the mainstem or the greater the resistance of material to be eroded, the greater the gradient advantage required for avulsion—hence the very high gradient ratios required for avulsion in cohesive (muddy) compared to noncohesive (sandy) systems. Thus, the critical gradient ratio necessary for avulsion is likely to vary depending on site boundary conditions, such as channel efficiency, bank and floodplain erodability, floodplain gradient, among others (Makaske, 2001; Törnqvist and Bridge, 2002).

The research literature generally focuses on the necessary conditions for distributary formation, while less attention has been given to predictors of distributary size (but see Edmonds and Slingerland, 2007; Syvitski and Saito, 2007). The paper presented here provides a case study of historical changes in the sizes (upstream inlet widths) of a set of delta distributaries, and relates these changes to larger scale changes in the planform geometry of the marsh distributary system. Slingerland and Smith's (1998) model of avulsion behavior is found to be consistent with observations in the sand-dominated Skagit Delta (Washington, USA). Moreover, slope ratios are shown to be correlated with distributary inlet width and bankfull cross-sectional area. These results are used to predict the likely medium-term (decades-scale) fate of a new distributary recently formed by the intersection of a meandering river channel with a preexisting blind tidal channel. This model of distributary dynamics is also used to predict the potential size and stability of river distributaries that have been proposed for restoration to improve delivery of sediment and seaward-migrating juvenile salmon to eroding and underutilized tidal marsh habitat (SRSC and WDFW, 2005).

2. Setting

2.1. Geographical context

With a mean annual discharge of 470 $m^3 s^{-1}$, the Skagit is the largest river draining into Puget Sound (Washington, USA), providing about 34% of the freshwater input to the Sound. Its 8544-km^2 watershed drains the Cascade Mountains of northwestern Washington State and southern British Columbia. Elevations in the basin range from sea level to 3285 m. Mean annual precipitation ranges from 80 cm in the lowlands to over 460 cm in the mountains. More than 90% of the 327-km^2 delta has been isolated from riverine and tidal influence by dikes and has been converted to agriculture and other uses (Collins et al., 2003). Likewise, many large historical distributaries have been isolated from the river by dikes and tidegates (Collins et al., 2003). The two principal river distributaries, the North and South Forks of the Skagit River, bound two sides of the 54-km^2 triangular Fir Island area of the delta with Skagit Bay on the third side (Fig. 1). Historical distributaries that once traversed Fir Island were isolated from the river as recently as the 1950s, so most of the remaining minor distributaries and associated undiked tidal wetlands are located at the mouths of the North and South Forks with relatively little marsh remaining along the bayward fringe of Fir Island between the North and South Fork outlets. Marsh sediments consist of organic-rich silt, silty clay, and fine sand; while unvegetated tidal flats are fine to medium sand. River distributary sediments generally consist of medium sand. Tides are semidiurnal with a maximum range of 4 m. The North Fork marsh, which is the focus of this study, is only one-third the area of the South Fork marsh, so the distributary network in the North Fork marsh is consequently less complex than that in the South Fork marsh. Additional details on the geomorphology, hydrodynamics, and ecology of the Skagit River estuary can be found in Hood (2006, 2007a) and Yang and Khangaonkar (2009).

2.2. Motivating observations and questions

As it enters Skagit Bay, the North Fork Skagit River distributary has two meander bends just downstream from where it is last constrained by levees on its south bank and a bedrock outcrop on its north bank. The concave bank of the upstream meander bend is bordered by sandy and silty marsh sediments, while the concave bank of the following bend is constrained by bedrock. Consequently, the unconstrained upstream meander bend has steadily eroded its concave bank over its documented history (since 1889), while the downstream bend has been stable (Fig. 1). While examining the sequence of historical maps and photos showing this meander history in early 2003, it became apparent that the upstream river meander would soon intersect a preexisting blind tidal channel that drained directly into Skagit Bay. This would cause an avulsion by annexation (*sensu* Slingerland and Smith, 2004) mediated by channel meandering, and the blind tidal channel would become a new distributary of the North Fork Skagit River.

Following an ~30-year flood event (3820 $m^3 s^{-1}$) in October 2003, a site visit was made in January 2004 to measure the distance separating the North Fork Skagit River and the blind tidal channel. The two channels were separated by as little as 7 m, but a small incised avulsion channel was now present connecting the North Fork to the formerly blind tidal channel (Fig. 2). The avulsion channel was 0.7 m wide for the upstream half of the reach, flaring to 2 m at its junction with the intersected marsh tidal channel. The depth was 0.2 m for the upstream 1.5-m length of channel and 1.0 m for the remaining 9.5-m of channel length. At this time, the blind channel intercepted by the newly incised avulsion was 0.75 m deep in the vicinity of the avulsion, and at low tide the channel was completely drained. Since then, the avulsion-captured channel has steadily eroded and is now in early 2010 about 2.5 m deep, permanently inundated, and can no longer be

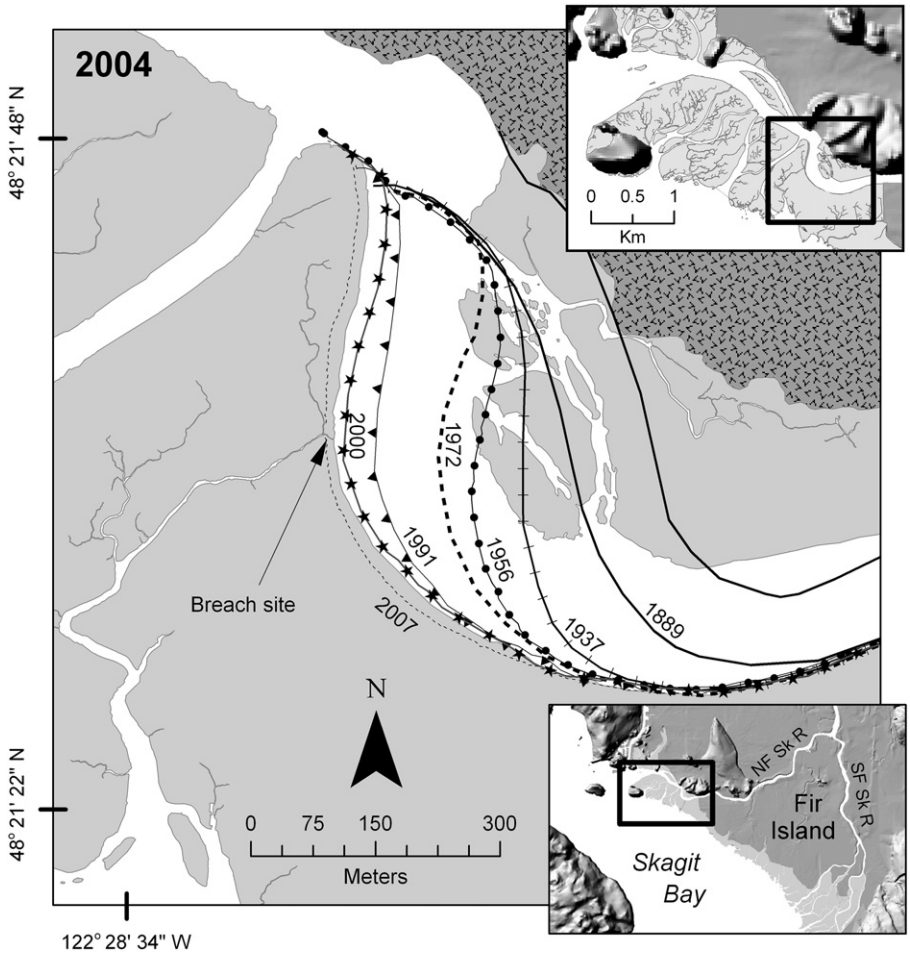

Fig. 1. Meander migration history of the North Fork Skagit River where it enters the remaining North Fork tidal marshes. The outlines of the historical channel banks are superimposed on the 2004 map; both banks of the 1889 channel are shown, but for clarity only the cutbanks are shown for the other historical channels. Tidal marshes are light grey; bedrock outcrop is checked. The breach site indicates where the river eroded into a preexisting blind tidal channel, converting its downstream reach into a new distributary. Upper inset shows medium-scale site context; lower inset shows large-scale context; tidal marshes are light grey, agriculture dark grey, water white, and hills are shaded-relief; NF Sk R = North Fork Skagit River, SF Sk R = South Fork Skagit River.

Fig. 2. Left photo: upstream end of an 11-m-long newly incised avulsion channel (foreground) connecting the North Fork Skagit River (background) to a previously blind tidal channel (not in the frame). Right photo: the same channel one year later. The log on the right bank is the same in both photos and indicates relative scale. The upstream end of the channel is 0.7 m wide in 2004 and 2.5 m wide in 2005. In January 2010, the most recent observation, it was 13 m wide.

waded at low tide. The natural question following these observations was how large could the new distributary channel become?

2.3. Management context

Historical distributaries across Fir Island (Fig. 3) were diked along their lengths circa 1897 to facilitate agricultural development in the delta. In the 1950s, to reduce dike maintenance costs and breaching risk, the distributaries were isolated from the North Fork Skagit River at their upstream ends by dams and from Skagit Bay at their downstream ends by tide gates. Isolation of the distributaries eliminated fluvial delivery of freshwater, sediment, and juvenile salmon to the marshes at the outlets of the former distributaries. Sediment starvation of the bay fringe marshes appears to have contributed to marsh erosion and loss of tidal channels (Hood, 2007b) with consequent ecological impacts, particularly for threatened Chinook salmon (*Oncorhynchus tshawytscha*) for whom tidal marsh channels are a critical rearing habitat. Restoration of these historical distributaries has been proposed to restore tidal marsh and help recover threatened Chinook salmon (SRSC and WDFW, 2005). However, Fir Island property owners have expressed concern that distributary restoration will risk full river avulsion and thereby threaten their property. To assess this risk and estimate the likely width of restored Fir Island distributaries, inferred distributary/mainstem (d/m) gradient ratios (see Section 3.1) were calculated for the isolated Fir Island distributaries using aerial photographs from 2004. Additionally, the 1937 aerial photographs and 1889 map were similarly analyzed as a test of the inferred d/m gradient ratio methodology.

3. Methods

3.1. Working hypothesis

The working hypothesis was that distributary width or cross-sectional area would be correlated with gradient advantage, i.e., with the distributary:mainstem ratio of water surface slopes. This would be consistent with the observation that distributary senescence (narrowing) is often due to gradient reduction during local delta progradation with flow switching to steeper distributaries (e.g., Coleman, 1988). It would also be a conceptual extension of Slingerland and Smith's (1998) model of avulsion behavior. This hypothesis was tested on the existing and historical distributary networks in the small delta of the North Fork Skagit River (Fig. 4). The distributary:mainstem slope ratio was represented by $(\Delta z_d/\Delta x_d)/(\Delta z_m/\Delta x_m)$, where Δz represented the water surface head and Δx the distance from the bifurcation point to the mainstem (m) or distributary (d) termini. Given that the water surface elevation at a bifurcation point is common to the mainstem and distributary flowpaths, then if one assumes the river and distributary termini end at approximately sea level and thus have similar water surface elevations, $\Delta z_d = \Delta z_m$ and the gradient ratio reduces to $\Delta x_m/\Delta x_d$, i.e., the d:m gradient ratio can be approximated by the m:d flowpath distance ratio, hereafter known as the inferred d/m gradient ratio. At low tide most of the distributaries have little if any flow, so the assumption $\Delta z_d = \Delta z_m$ is meaningful mostly near high tide. This simplification allows gradient ratios to be estimated from geographic information system (GIS) analysis of aerial photographs.

3.2. Analysis of aerial photography

GIS was used to compare true color (2009, 2007 and 2000) and infrared (2004) digital orthophotos and black and white historical aerial photographs (1937, 1956, 1972 and 1991). The 2007 and 2009 true color orthophotos had 30-cm pixels, were 1:12,000 scale, and were flown in April during mid-tide (+1.5 and +2 m MLLW, respectively) when large sandbars and higher sandflats were exposed. Tidal marsh channels as small as 0.6 m wide were distinguishable in the 2007 and 2009 photographs because marsh vegetation was either ankle high or sparse at this time of year. Details on the other aerial photographs have been reported previously (Hood, 2006); but in brief, channels as narrow as 0.3, 0.6, and 1.0 m could be resolved for the 2004, 2000, and older photos, respectively. A georeferenced 1889 U.S. Coast and Geodetic T-sheet of the Skagit Delta (Puget Sound River History Project, University of Washington) allowed location of historical shorelines of the North Fork Skagit River.

All historical photographs were rectified relative to the 2000 orthophotos using reference points (e.g., road intersections) visible in both historical and recent photographs; mean absolute rectification errors were <2.6 m. For all photographs, tidal channel margins and other shorelines were manually digitized in the GIS. Shorelines were defined by the abrupt transition from vegetated to unvegetated intertidal areas. Distinct photo-signatures almost always allowed vegetated and unvegetated areas to be clearly distinguished. Further

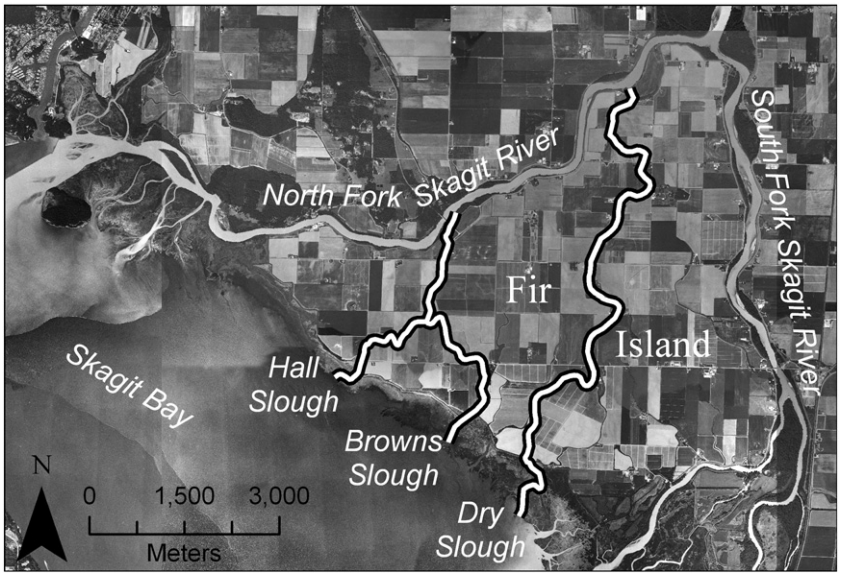

Fig. 3. Location of historical Fir Island distributaries (Browns–Hall Slough and Dry Slough), which are now isolated from the North Fork Skagit River by dikes and from Skagit Bay by tide gates. Distributary widths are exaggerated for graphic clarity.

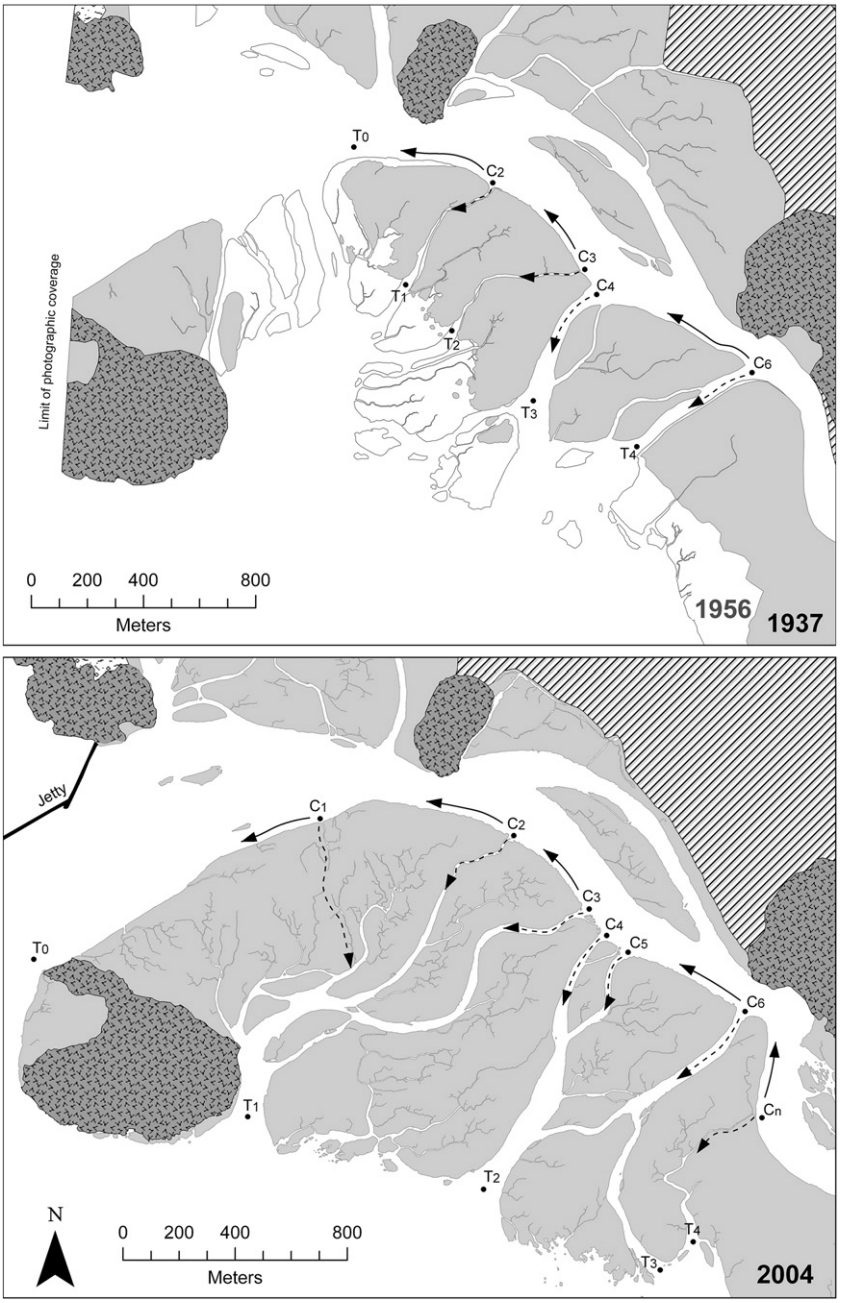

Fig. 4. Planforms of the North Fork marsh/distributary system. Cross-hatched areas are farmland, checked areas are bedrock outcrops, light gray is tidal marsh in 1937 (top frame) and 2004 (bottom frame), gray outline indicates 1956 tidal marsh (top frame), white areas are channels and bay. T_0 is the river terminus used to determine the mainstem flow path length from a bifurcation. T_1–T_4 are the termini for distributaries of the North Fork Skagit River. C_1–C_6 are the distributary channel bifurcation points. Planforms for 1972 and 1991 are not shown but are similar to 2004, except the marshes have prograded less into the bay so the distributary lengths are shorter.

details of the photographic analysis, including estimation of rectification and digitization error, have been previously described (Hood, 2004, 2006).

Most distributary inlets were broadly funnel-shaped (tapering downstream for several tens of meters before sustained bayward widening of the rest of the channel), so definition of the precise location of the distributary inlet could often be an arbitrary decision to which estimates of inlet width were sensitive. Consequently, distributary channel widths were measured in the GIS at the narrowest cross section in the upstream half of the distributary. This was typically very near the distributary bifurcation from the North Fork mainstem.

Distributary and river termini were defined as occurring at the seaward limits of the tidal marsh through which the channels passed. In most instances distributaries ended at an abrupt and straight marsh margin so that their seaward limit was unambiguous. However, in some instances one or both channel banks flared sharply outwards near the channel mouths; in these cases the termini were defined as occurring at the point at which the flaring began.

3.3. Field surveys

Distributary cross sections were surveyed with a laser level at low tide in August 2006 near the upstream inlets. Elevations for each cross section were measured relative to an arbitrary zero, set at the lowest vegetated point surveyed within a cross section, which approximated mean high water (MHW). Bankfull cross-sectional area was calculated up to the lower of the two banks on a cross section. The upstream inlet

width and depth of the newly avulsed distributary were measured annually from 2004 to 2009, initially with a survey rod to the nearest 0.1 m; but as the channel width began to exceed the 7-m length of the rod, a laser range finder (Impulse LR by Laser Technology Inc., Englewood, CO) was used to measure channel width to the nearest 0.5 m. Because of shoreline irregularities, channel width was estimated from the mean of five measurements in the general vicinity of the channel inlet.

Tide gages (Levelogger by Solinst Canada Ltd., Ontario, Canada) were deployed from mid-July through mid-August 2008 to provide field-based estimates of water surface slope ratios that could be compared with GIS-based estimates. One tide gage was maintained at the terminus of the North Fork throughout the gauging period, while two other tide gages were rotated among distributaries to the North Fork Skagit River to simultaneously measure water levels at the inlet and outlet of a distributary during each two- or three-day rotation (Fig. 4). Water levels were logged at 6-minute intervals during spring tides and typical seasonal river flow (315 $m^3\ s^{-1}$). Tide gages were leveled relative to one of four temporary benchmarks (metal fence stakes or pvc pipes sunk to 1.5 m depth) distributed throughout the North Fork study area, and surveyed with RTK-GPS (Leica SmartRover; 3-cm vertical and horizontal accuracy).

3.4. Statistical analysis

Minimum distributary widths were regressed against inferred d/m gradient ratio for each set of historical photos. Regression slopes and intercepts were compared among photo years by analysis of covariance (ANCOVA) following Zar (1999). When regression slopes and intercepts were not significantly different among groups, a common regression equation was calculated from the ANCOVA. The criterion for statistical significance was $p<0.05$. The confidence interval for estimating Y_i from a regression analysis was calculated using the standard error for single measurement at X_i (Zar, 1999, pg. 341).

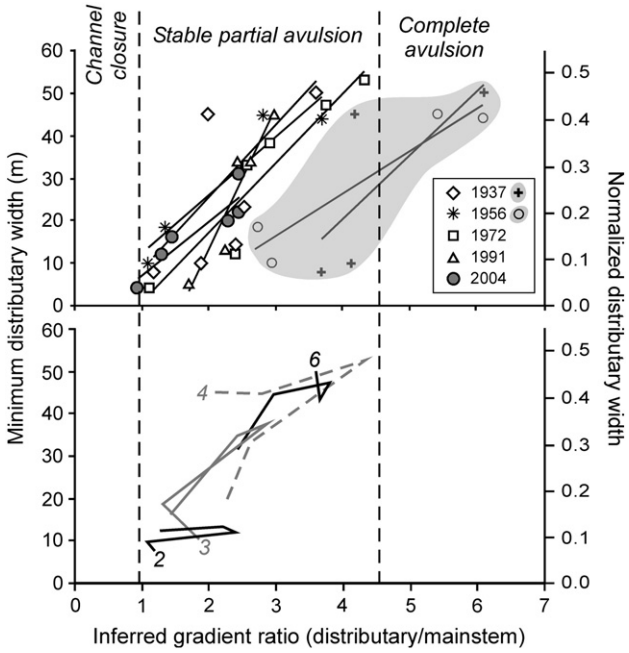

Fig. 5. Top frame: observed relationship between distributary widths for the North Fork Skagit River distributaries and water surface gradient ratios inferred from flow path lengths measured in historical aerial photos. The shaded points illustrate results for the 1937 and 1956 channels when changes in river flow path length from marsh progradation were not accounted for, i.e., when the 1972–1991–2004 river terminus was used to calculate the 1937 and 1956 river flow path lengths. Bottom frame: trajectories of four distributary channels from 1937 to 2004. The beginning of each trajectory is marked by a numbered label corresponding to the numbered distributaries in Fig. 4. Thresholds for channel closure (failed avulsion) and complete avulsion are marked by vertical dashed lines and are based on Slingerland and Smith (1998, 2004). The single 2004 point below the channel closure threshold was a historical distributary that has recently closed near its midpoint to form two blind tidal channels, one draining north into the North Fork Skagit River and the other draining south into Skagit Bay.

4. Results

4.1. Distributary gradient ratios and dynamics

System geometry was significantly different for 1937 and 1956 compared to subsequent years. Significant marsh development lengthened the mainstem North Fork flow path from 1956 to 1972 (Fig. 4). Additionally, a jetty was constructed after 1937 on the north side of the North Fork mainstem that likely contributed to lengthening its flow path. Consequently, analysis of gradient advantage assumed two different river termini depending on planform geometry. Distributary outlet locations and flow path lengths changed for each historical photograph because of persistent marsh progradation. Bifurcation locations were relatively constant during the historical record, except where new distributaries were formed during marsh progradation.

For all years examined, inferred d/m gradient ratios predicted minimum distributary widths relatively well (Fig. 5). The lowest R^2 was 0.61 for the 1937 data points, but ranged from 0.83 to 0.90 for the other year-specific regression lines. With the river terminus adjusted to account for marsh progradation from 1937 and 1956 to later years, ANCOVA indicated no statistical difference in regression slopes for all photo years ($F_{4,\ 15}=1.047$) and no difference in regression intercepts ($F_{4,\ 19}=1.205$). The lack of statistical distinction between years indicates constancy in the effect of inferred d/m gradient advantage even though system geometry varied over time from progradational changes in either mainstem flow path length or distributary flow path lengths or both. To investigate the sensitivity of this planform analysis to the location of the river terminus and to compare system geometry between 1937−1956 and 1972−1991−2004, the ANCOVA was repeated using the 1972–1991–2004 river terminus to calculate the gradient ratios for the 1937 and 1956 planform geometries, i.e., the same 2004 river terminus was used for all photo years. Under this condition, the 1937 and 1956 points plotted separately from the other photo years (Fig. 5, shaded zone). While the 1937 and 1956 regression slopes did not differ from those of the other photo years ($F_{4,\ 15}=1.632$), their intercepts did ($F_{4,\ 19}=4.746$, $p<0.02$). Furthermore, the gradient ratios of some of the larger 1937 and 1956 distributaries ranged from 5.3 to 6.1, over the threshold of ~5 that the model of Slingerland and Smith (1998, 2004) predicted would result in complete avulsion, contrary to observed North Fork distributary history. This contrast with the first ANCOVA results reinforces the earlier inference that the river terminus location was significantly affected by marsh progradation in the first half of the twentieth century.

The best estimate of the relationship between inferred d/m gradient ratio and distributary inlet width should probably be based on the 2004 data, which were derived from high resolution infrared orthophotographs, thus minimizing channel width measurement error. Consequently, further calculations requiring channel width estimation from inferred d/m gradient ratios utilized the 2004 regression equation: $w=12.7r_g-5.4$, where w is distributary inlet width and r_g is inferred d/m gradient ratio. When the 2004 distributary widths were normalized by the width of the mainstem North Fork Skagit River just upstream of the large migrating meander bend (110 m), the regression equation became $w_n=0.1156r_g-0.0495$, where w_n is normalized distributary inlet width. This normalized regression relationship may be generally applicable to similar sand-dominant distributary networks in river-dominated deltas.

Generally, individual channel widths alternately grew and shrank as first the river terminus and then the distributary termini moved seaward from marsh progradation (Fig. 5). Seaward relocation of the river terminus from 1937 to 1956 caused the river flow path length to increase by about 1250 m, while distributary lengthening was relatively modest during this time. Consequently, the gradient advantage of the distributaries increased and their channels widened. After the river terminus stabilized from 1956 to the present, the distributaries continued to lengthen from marsh progradation, so distributary gradient advantage steadily declined and the distributaries narrowed. The inferred d/m gradient ratios observed over all photo years ranged from 0.93 to 4.29. The lowest observed gradient ratio pertained to channel 1 in 2004, which field observations confirm has recently closed near its mid-length to form two blind tidal channels, one draining north into the North Fork mainstem and one draining south into Skagit Bay (C_1 in Fig. 4). These observations are consistent with theoretical predictions for channels that, like the Skagit River, have suspended sediment loads consisting of medium sand, where stable partial avulsions are expected for gradient ratios between 1 and 5 and where channel closure is expected for ratios below 1 (Slingerland and Smith, 2004).

While distributary cross sections were not available for the historical period, they were field-surveyed in 2007 near the distributary inlets (Fig. 6). The regression of distributary inlet bankfull cross-sectional area on inferred d/m gradient ratio produced $R^2 = 0.95$ (Fig. 7), which was significantly higher than the sample of regression

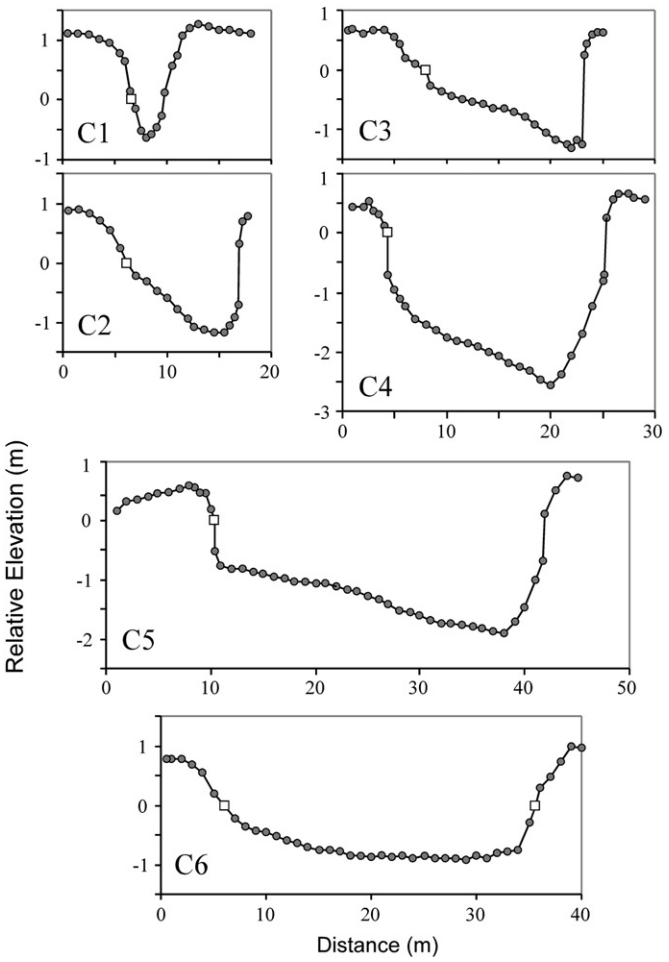

Fig. 6. Distributary inlet cross sections. Graph labels correspond to channel inlet locations in Fig. 3. Open square marks the lower limit of vegetation and corresponds approximately to mean high water (MHW). Elevations are relative to MHW.

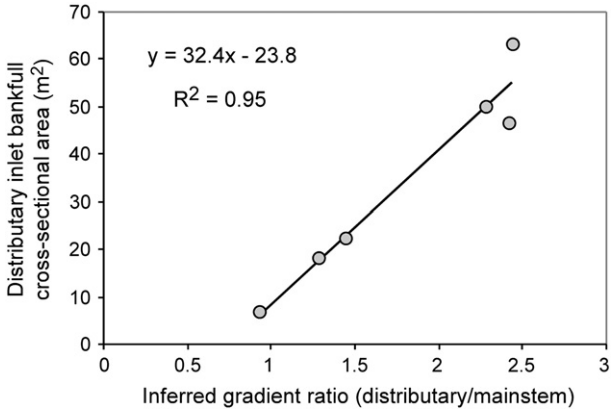

Fig. 7. Relationship between inferred d/m gradient ratio and bankfull cross-sectional area of the North Fork distributaries.

coefficients produced from the historical photo analysis of distributary inlet width (one-sided $t = 2.418$, $df = 4$, $p < 0.05$).

Tide gage measurements indicated that maximum observed ebb tide hydraulic head varied from 17 cm for the distributary channel nearest the river outlet (C_1) to 57 cm for the new avulsion (C_n), with corresponding maximum water surface gradients of 0.00014 and 0.00082, respectively. These values were constrained by hydraulic control at the distributary outlets. At low tide, the high sandflats at the mouths of the shallow distributary channels act as a dam—or hydraulic control. Hydraulic control limits the extent to which the water level in the distributaries can drop at low tide; water ponds in the shallow channels, sometimes forming discontinuous pools in the sandy beds of the distributaries. Comparable hydraulic control is not present for the deeper river channel. Consequently, at low tide the river gradient was greater than the distributary gradients, and the low tide d/m gradient ratios were <1 (Fig. 8). In contrast, the new distributary was sufficiently deep that hydraulic controls were usually not evident and that the d/m gradient ratio rarely dipped below 1 at low tide. The d/m gradient ratio peaked early in the ebb tides, and the means of the top 10 ebb-tide gradient ratio values for each distributary were comparable to the inferred d/m gradient ratios derived from GIS analysis of distributary planform (Fig. 9).

4.2. Fate of the new distributary

Currently, the newly avulsed distributary (C_n) has an inferred d/m gradient ratio of 4.9, which is near Slingerland and Smith's (1998, 2004) theoretical threshold of ~5 between partial and complete avulsion. However, this ratio should decline as the marsh progrades near the distributary terminus, as the new distributary can now deliver fluvial sediment directly to this area. The faster the channel lengthens through marsh progradation, the lower its inferred d/m gradient ratio will become and the narrower the channel inlet will be when its erosional widening peaks. Thus, several questions follow: how quickly will the new distributary widen and lengthen, and consequently, how wide can the channel become? From annual measurements of channel width from 2004 to 2010, the rate of channel widening was estimated to be 2.3 m/year with a 95% confidence interval of 1.6 to 3.0 m. The rate of potential channel lengthening through marsh progradation was estimated from historical aerial photographs. ANCOVA did not detect significant differences in channel lengthening among the four channels present throughout the photographic record ($F_{8,\ 11} = 0.93$), so that the mean rate of channel lengthening was estimated as 10.5 m/year with a 95% confidence interval of 7.1 to 13.9 m/year (Fig. 10). The likely maximum future width of the new distributary channel was estimated from the intersection of observed channel widening rates and predictions of channel width from inferred d/m ratios (as

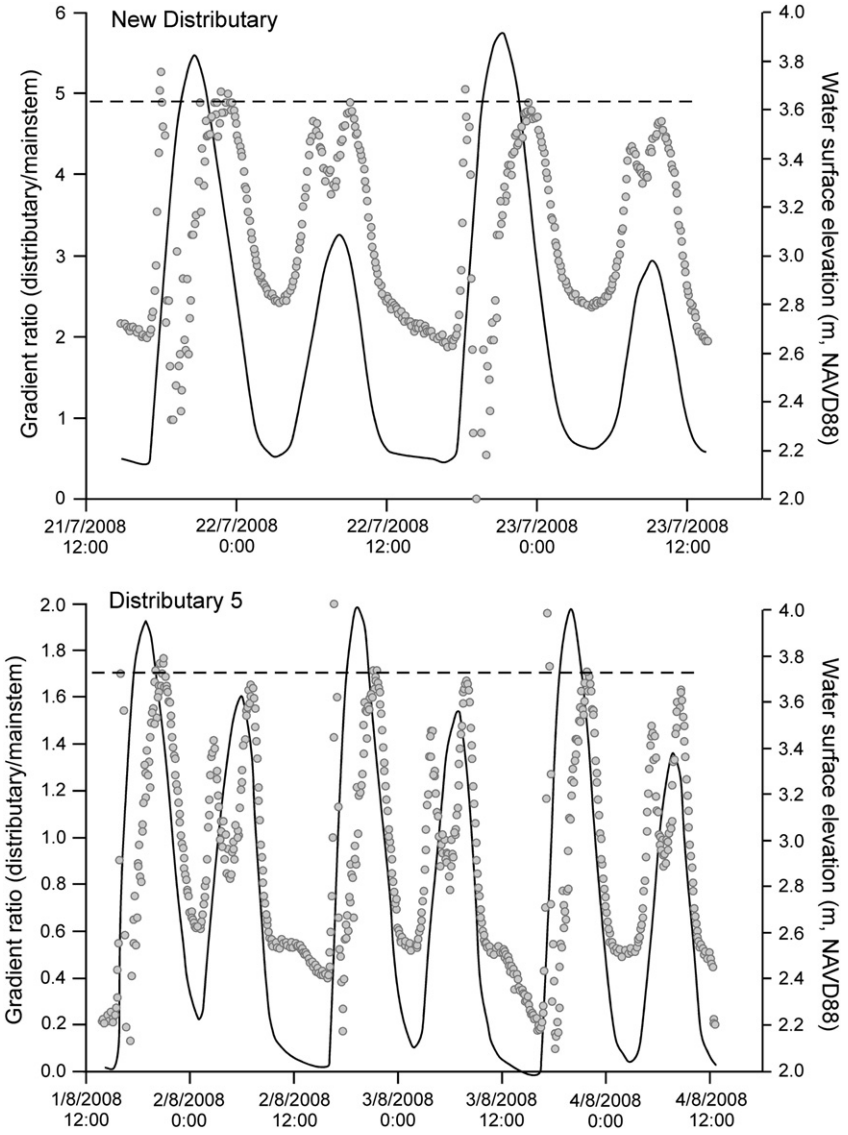

Fig. 8. Distributary:mainstem channel surface water gradient ratios (filled circles) derived from water level loggers located at the distributary bifurcation point and at river and distributary termini. The tide at the river terminus (solid line, right axis) is shown for reference. Dashed horizontal lines indicate the mean of the top 10 ebb tide *d*/*m* gradient ratio values.

described above) where the length of the new distributary was assumed to increase by 10.5 m/year, as observed for other distributaries in the historical record. This assumes no significant changes in river sediment load and associated marsh progradation rates in the next few decades compared to the past few decades. The intersection of these two relationships (Fig. 11) suggests that the new avulsion

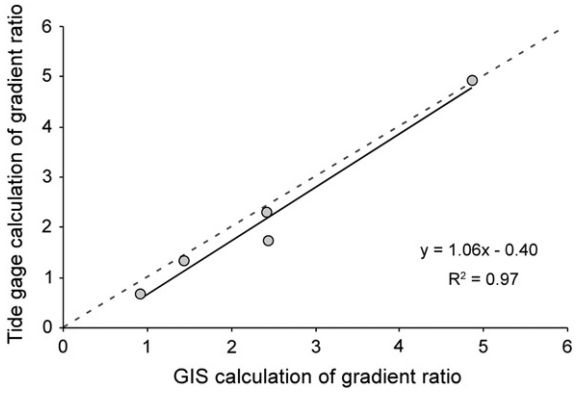

Fig. 9. Comparison of GIS-based and tide gage-based estimates of *d*/*m* gradient ratio. Dashed line is 1:1 line along which a perfect match between the GIS and tide gage calculations should ideally align. Tide gage values are the mean of the top 10 values occurring during the observed ebb tide peaks in gradient ratios.

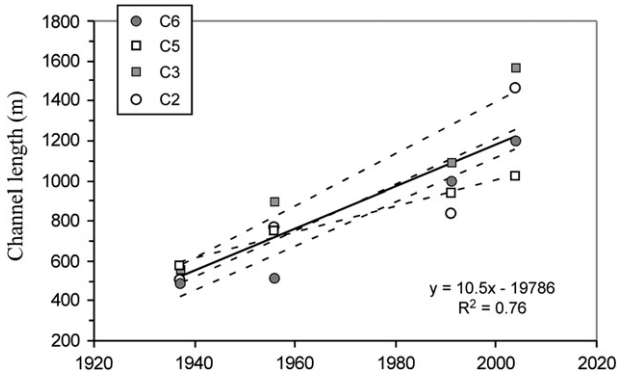

Fig. 10. Channel lengths for four North Fork distributaries present throughout a chronosequence of historical aerial photographs. Dashed lines are linear fits for each channel. The solid line is the pooled regression used to estimate mean channel lengthening rate. Channel labels are the same as for distributary inlets in Fig. 3.

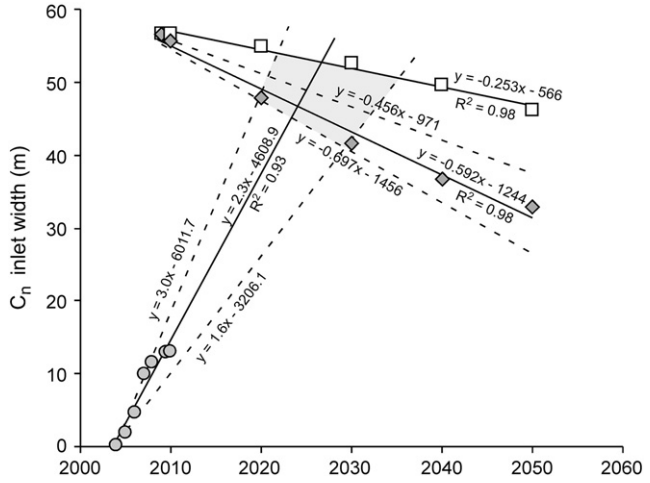

Fig. 11. Prediction of the maximum future width of the new North Fork distributary channel from the intersection of observed rates of channel widening and predictions of channel width derived from inferred d/m gradient ratios using two scenarios of marsh progradation. The extrapolation of the observed avulsion widening trajectory (filled circles on solid regression line) is bounded by trajectories (dashed lines) based on the 95% confidence intervals of the estimated widening rate. Channel width predictions from inferred d/m gradient ratios assuming constant channel lengthening of 10.5 m/year (filled diamonds on solid regression line) are bounded by trajectories (dashed lines) based on the 95% confidence intervals of the channel lengthening rate. The channel width predictions derived from inferred d/m gradient ratios assuming a scenario of initially slow and slowly increasing channel lengthening are represented by open squares on solid the regression line. The gray trapezoid bounds the likely peak inlet width and date of the newly avulsed distributary.

channel will widen until 2023 when it reaches a maximum width of 47 m and has an inferred d/m gradient ratio of 4.1, after which the channel will begin to narrow again as it continues lengthening and the inferred d/m ratio continues to decline. The 95% confidence intervals in the estimates of channel widening and lengthening rates were used similarly to bound the predicted time and magnitude of peak channel width. This indicated the channel would likely continue widening until sometime between 2020 and 2032, while channel width would peak between 41 m (with a gradient ratio of 3.7) and 51 m (with a gradient ratio of 4.4). However, the assumption of constant channel lengthening is simplistic. In the case of the new avulsion, the rate of sediment delivery to its terminus will likely increase over time as the channel widens and carries greater flow. If one assumes conservatively that the rate of channel lengthening for the new avulsion will initially be slow and increase slowly every decade (e.g., 2 m/year in the first decade, 3 m/year in the second, 4 m/year in the third, etc.), then the new avulsion channel widens until 2026 when it reaches a maximum width of 53 m and has a gradient ratio of 4.6. Given the 95% confidence interval on the estimated rate of observed channel widening, under this scenario the prediction bounds increase to 2035 for the year at which the channel will reach a maximum width and to 54 m for maximum width with a gradient ratio of 4.7. In comparison, the largest distributary in the North Fork is currently 31 m wide, while the North Fork mainstem is 130 m wide in the vicinity of the new avulsion. The widest distributary observed in the historical aerial photos was 53 m wide in 1972, comparable to the maximum estimate for the new avulsion channel.

4.3. Application to restoration planning

Fir Island distributary inlet width predictions derived from the 1937 inferred d/m gradient ratios were compared to inlet widths observed in the 1937 aerial photographs. This comparison assumed dikes bordering the 1937 distributaries had not encroached on the original predevelopment distributary channels so that the observed channel widths reflected an approximate morphological equilibrium. Comparison of the 1937 and 1889 planform measurements indicated little if any difference in inferred d/m gradient ratios and similar distributary inlet widths. This suggests the much higher resolution 1937 photographs were a reasonable indicator of distributary planform conditions depicted in the 1889 map, particularly with regard to reliably measuring 1889 channel inlet widths. Observed historical inlet widths were comparable to widths predicted from inferred d/m gradient ratios for Browns–Hall Slough, but Dry Slough was underpredicted (Table 1). Underprediction of Dry Slough width may be due to channel shoaling as suggested by the distributary's name (dating to the 1889 map) and by a clearly mapped shoal at the inlet of the 1889 distributary; the Dry Slough inlet was coincident with a North Fork mainstem point bar on the convex side of a meander in 1889, but was anthropogenically relocated downstream after the 1950s.

Compared to the historical condition, the inferred d/m gradient ratios have increased slightly for the 2004 distributaries because the river terminus has moved seaward as a result of marsh progradation since 1937, while no progradation has occurred at the Fir Island distributary termini. Consequently, the predicted inlet widths were greater for the 2004 distributaries than for those of 1937, but the predicted widths only increased from 14 to 19 m for Browns–Hall Slough and from 9 to 10 m for Dry Slough. The inferred d/m gradient ratios for the Fir Island distributaries were all <2, well below Slingerland and Smith's (1998, 2004) full avulsion threshold of ~5. These results suggest distributary restoration would not incur significant risk of complete river avulsion and that distributary widening from historic conditions would be minor.

5. Discussion

The avulsion model of Slingerland and Smith (1998, 2004) was developed with fluvial systems in mind, but it apparently also applies in a tidally influenced river delta. Consistent with hydraulic geometry relating channel cross-sectional area and water surface slope to discharge or tidal prism (Myrick and Leopold, 1963; Leopold et al., 1964; Rinaldo et al., 1999; Williams et al., 2002), gradient advantage predicted present-day distributary bankfull cross-sectional area very well, and bankfull conditions occur with every high tide. Additionally, ebb tide velocities generally peak as the tide drops below the marsh surface (French and Stoddart, 1992), i.e., at bankfull conditions; and the tide gage data indicate that this is approximately the point in time at which distributary gradient advantage is maximal. Thus, the tidal Skagit Delta example indicates that even a transient, although recurring, gradient advantage occurring for relatively brief moments

Table 1
Application of inferred d/m gradient ratio analysis to potential Fir Island distributary restoration: comparison of observed and predicted distributary inlet widths for open historical distributaries and isolated modern distributary remnants.[a] Error estimates refer to the 95% confidence limits of the predictions.

	Inferred d/m gradient ratio	Predicted inlet width (m)	Observed inlet width (m)
Browns Slough (1889)	1.31	11 ± 13	13
Hall Slough (1889)	1.54	14 ± 13	13
Dry Slough (1889)	1.11	9 ± 14	13
Browns Slough (1937)	1.35	12 ± 13	14
Hall Slough (1937)	1.55	14 ± 13	14
Dry Slough (1937)	1.12	9 ± 14	16
Browns Slough (2004)	1.50	14 ± 13	4[b]
Hall Slough (2004)	1.95	19 ± 13	4[b]
Dry Slough (2004)	1.22	10 ± 14	4[b]

[a] Note that Browns and Hall Sloughs bifurcate from a shared trunk channel, so the larger predicted inlet width of the pair was assumed to be the relevant comparison to the observed inlet width of the trunk.

[b] Ground observations indicated these narrow widths were due to anthropogenic channel manipulations or to channel infilling by sediments eroded from farm fields.

on ebbing tides is sufficient to influence distributary geometry. Moreover, the planform geometry of the North Fork Skagit River was consistent with the Slingerland and Smith (1998, 2004) avulsion model throughout the delta's progradational history. For all time periods examined, the active distributaries had inferred d/m gradient advantages between 1 and 5, i.e., they were similar to stable partial avulsions. Likewise, the critical avulsion threshold for complete avulsion in this system appears to be at least 5, as predicted by theory, while the only distributary to senesce did so when its inferred d/m gradient advantage fell below 1. Furthermore, inferred d/m gradient advantage was found to predict distributary size, a result not anticipated by Slingerland and Smith (1998, 2004). The effect of gradient advantage on distributary inlet width was constant even though system geometry varied over the past century from progradational changes in mainstem flow path length, distributary flow path lengths, or both. Individual channel widths alternately grew and shrank as first the river terminus and then the distributary termini moved seaward because of marsh progradation.

Except for the previously described 2004 avulsion through meander annexation of a preexisting blind tidal channel, the historical aerial photos do not document distributary formation through avulsions across preexisting tidal marsh. Instead, the North Fork distributaries appear to form concurrently with marsh progradation (Hood, 2006). Yet regardless of the mechanism generating the North Fork distributaries, gradient advantage is clearly implicated in distributary maintenance by determining channel width and consequently channel fate, i.e., persistence or senescence. More generally, distributary channel senescence (infilling, narrowing, and abandonment) in mature deltas is commonly attributed to loss of gradient advantage (e.g., Coleman, 1988). Thus, mature deltas, regardless of the origin of their distributary network, should express correlations between gradient advantage and distributary width.

The North Fork Skagit Delta has a very simple geometry, consisting of a mainstem channel with several distributaries branching from one side of the mainstem. Each distributary has few if any secondary distributaries. Consequently, this simple geometry is perhaps ideally suited to isolate and illustrate the effect of distributary gradient advantage on distributary width and fate. More complicated anastomosing tidal distributary networks are likely affected by additional variables, particularly network-scale indirect hydrodynamic effects (e.g., Yang et al., 2010). Even within the limited scope of local scale bifurcation geometries, Kleinhans et al. (2008) found that in addition to gradient advantage avulsion fate depends on the location of the avulsion on the concave versus convex side of a meander bend, resistant lips at the entrance of the new channel, the location of sandbars near the bifurcation, and interactions between these and other variables, such as tidal influence. Thus, with more complicated network geometries, gradient advantage will likely be only one of several influences on distributary dynamics.

6. Conclusions

(i) North Fork Skagit River distributary dynamics are consistent with the Slingerland and Smith model of avulsion dynamics. Inferred d/m gradient ratios observed over all photo years ranged from 0.93 to 4.29, in agreement with theoretical predictions for stable partial avulsions when gradient ratios range from 1 to 5 for channels dominated by medium sand (Slingerland and Smith, 2004). The lowest observed gradient ratio pertained to a channel that, in accordance with model predictions, has recently closed near its mid-length to form two blind tidal channels: one draining north into the North Fork mainstem and one draining south into the bay.

(ii) The Slingerland and Smith avulsion model was extended to predict distributary inlet (upstream) width and bankfull cross-sectional area. The effect of inferred d/m gradient advantage on distributary inlet width was constant even though system geometry varied over time because of marsh progradation causing changes in mainstem and distributary flow path lengths.

(iii) Distributary/mainstem gradient ratios calculated from planform channel geometry were correlated with peak water surface gradient ratios calculated from tide gage measurements. Tide gage-measured d/m gradient ratios peaked early in the ebb tides during bankfull conditions when ebb tide velocities would have been maximal. The evident relationship between bankfull ebb tide flow and d/m gradient ratios, the conformity of the North Fork distributary channel system to the geometry predicted by the Slingerland and Smith avulsion model, and the short timescales characteristic of sandy tidal flat channel dynamics suggest that sandy tidal flats could be a useful model system to study channel avulsion in tidal environments.

(iv) The new avulsion channel (C_n) will likely continue widening at a mean annual rate of 2.3 m until it reaches a width of 41 to 54 m between 2020 and 2035, after which continued marsh progradation and channel lengthening would cause the channel to narrow. This assumes no significant changes in river sediment load in the next few decades compared to the past few decades. In comparison, the largest distributary in the North Fork is currently 31 m wide, while the North Fork mainstem is 130 m wide in the vicinity of the new avulsion. The widest distributary observed in the historical aerial photos was 53 m wide in 1972, comparable to the maximum estimate for the new avulsion channel.

(v) Applying this form of analysis to North Fork Skagit River distributaries, which have been dammed in the course of agricultural development, suggests that their restoration to stabilize eroding marshes and recover salmon migration pathways would be feasible without significant risk of full river avulsion.

Acknowledgements

Thanks to Tim Beechie, Jeff Phillips, Bart Makaske and three anonymous referees for reviewing the draft manuscript. This work was supported in part by the Office of Naval Research (Tidal Flat Dynamics Departmental Research Initiative, Grant # N00014-08-1-1008).

References

Aslan, A., Autin, W.J., Blum, M.D., 2005. Causes of river avulsion: insights from the late Holocene avulsion history of the Mississippi River, USA. Journal of Sedimentary Research 75, 650–664.

Coleman, J.M., 1988. Dynamic changes and processes in the Mississippi River delta. Geological Society of America Bulletin 100, 999–1015.

Collins, B.D., Montgomery, D.R., Sheikh, A.J., 2003. Reconstructing the historical riverine landscape of the Puget lowland. In: Montgomery, D.R., Bolton, S., Booth, D.B., Wall, L. (Eds.), Restoration of Puget Sound Rivers. University of Washington Press, Seattle, pp. 79–128.

Edmonds, D.A., Slingerland, R.L., 2007. Mechanics of river mouth bar formation: implications for the morphodynamics of delta distributary networks. Journal of Geophysical Research 112, F02034, doi:10.1029/2006JF000574.

French, J.R., Stoddart, D.R., 1992. Hydrodynamics of salt marsh creek systems: implications for marsh morphological development and material exchange. Earth Surface Processes and Landforms 17, 235–252.

Hood, W.G., 2004. Indirect environmental effects of dikes on estuarine tidal channels: thinking outside of the dike for habitat restoration and monitoring. Estuaries 27, 273–282.

Hood, W.G., 2006. A conceptual model of depositional, rather than erosional, tidal channel development in the rapidly prograding Skagit River Delta (Washington, USA). Earth Surface Processes and Landforms 31, 1824–1838.

Hood, W.G., 2007a. Large woody debris influences vegetation zonation in an oligohaline tidal marsh. Estuaries and Coasts 30, 441–450.

Hood, W.G., 2007b. Scaling tidal channel geometry with marsh island area: a tool for habitat restoration, linked to channel formation process. Water Resources Research 43, W03409, doi:10.1029/2006WR005083.

Kleinhans, M.G., Jagers, H.R.A., Mosselman, E., Sloff, C.J., 2008. Bifurcation dynamics and avulsion duration in meandering rivers by one-dimensional and three-dimensional models. Water Resources Research 44, doi:10.1029/2007WR005912 WO8454.
Leopold, L.B., Wolman, M.G., Miller, J.P., 1964. Fluvial Processes in Geomorphology. W.H. Freeman and Company, San Francisco.
Lorang, M.S., Whited, D.C., Hauer, F.R., Kimball, J.S., Stanford, J.A., 2005. Using airborne multispectral imagery to evaluate geomorphic work across floodplains of gravel-bed rivers. Ecological Applications 15, 1209–1222.
Makaske, B., 2001. Anastomosing rivers: a review of their classification, origin and sedimentary products. Earth-Science Reviews 53, 149–196.
Myrick, R.M., Leopold, L.B., 1963. Hydraulic geometry of a small tidal estuary. Geological Survey Professional Paper, 422-B.
Pasternack, G.B., Brush, G.S., Hilgartner, W.B., 2001. Impact of historic land-use change on sediment delivery to an estuarine delta. Earth Surface Processes and Landforms 26, 409–427.
Rinaldo, A., Fagherazzi, S., Lanzoni, S., Marani, M., Dietrich, W.E., 1999. Tidal networks: 3. Landscape-forming discharges and studies in empirical geomorphic relationships. Water Resources Research 35, 3919–3929.
Slingerland, R., Smith, N.D., 1998. Necessary conditions for a meandering-river avulsion. Geology 26, 435–438.
Slingerland, R., Smith, N.D., 2004. River avulsions and their deposits. Annual Review of Earth and Planetary Science 32, 257–285.
Skagit River System Cooperative (SRSC), Washington Department of Fish and Wildlife (WDFW), 2005. Skagit Chinook Recovery Plan. Skagit River System Cooperative, LaConner, WA. Available online: www.skagitcoop.org.
Stouthamer, E., Berendsen, H.J.A., 2007. Avulsion: the relative roles of autogenic and allogenic processes. Sedimentary Geology 198, 309–325.
Syvitski, J.P.M., 2008. Deltas at risk. Sustainability Science 3, 23–32.
Syvitski, J.P.M., Saito, Y., 2007. Morphodynamics of deltas under the influence of humans. Global and Planetary Change 57, 261–282.
Syvitski, J.P.M., Kettner, A.J., Correggiari, A., Nelson, B.W., 2005. Distributary channels and their impact on sediment dispersal. Marine Geology 222–223, 75–94.
Törnqvist, T.E., Bridge, J.S., 2002. Spatial variation of overbank aggradation rate and its influence on avulsion frequency. Sedimentology 49, 891–905.
Williams, P.B., Orr, M.K., Garrity, N.J., 2002. Hydraulic geometry: a geomorphic design tool for tidal marsh channel evolution in wetland restoration projects. Restoration Ecology 10, 577–590.
Yang, Z., Khangaonkar, T., 2009. Modeling tidal circulation and stratification in Skagit River estuary using an unstructured grid ocean model. Ocean Modelling 28, 34–49.
Yang, Z., Khangaonkar, T., Calvi, M., Nelson, K., 2010. Simulation of cumulative effects of nearshore restoration projects on estuarine hydrodynamics. Ecological Modelling 221, 969–977, doi:10.1016/j.ecolmodel.2008.12.006.
Zar, J.H., 1999. Biostatistical Analysis. Prentice Hall, Englewood Cliffs, NJ.